Vol. 77: 11–22, 2016
doi: 10.3354/ame01784

AQUATIC MICROBIAL ECOLOGY
Aquat Microb Ecol

Published online April 25

Bacterial enhancement of gel particle coagulation in seawater

Yosuke Yamada[1], Hideki Fukuda[1], Yuya Tada[1,2], Kazuhiro Kogure[1], Toshi Nagata[1,*]

[1]Atmosphere and Ocean Research Institute, The University of Tokyo, 5-1-5 Kashiwanoha, Kashiwa-shi, Chiba 277-8564, Japan

[2]*Present address:* Faculty of Environmental Earth Science, Hokkaido University, North 10 West 5, Kita-ku, Sapporo 060-0810, Japan

ABSTRACT: Gel-like particles are ubiquitous in marine environments, affecting global carbon cycles, but the mechanisms controlling gel particle coagulation in seawater are not entirely clear. We investigated whether marine bacteria enhance the coagulation of gel particles. Gel particles composed of polysaccharides with an equivalent spherical diameter (ESD) of 0.01 cm were suspended in seawater contained in rotating tubes to examine time course changes in particle ESD and abundance. Marine bacterial assemblages strongly enhanced the coagulation of gel particles into large aggregates (ESD, 0.1 to 1 cm) over a period of 24 to 96 h. Catalyzed reporter deposition fluorescence *in situ* hybridization revealed that one group of bacteria that grew rapidly was affiliated with the genus *Pseudoalteromonas*. Experiments using *Pseudoalteromonas* spp. isolates indicated that 6 of 11 isolates enhanced gel particle coagulation. This enhancement differed greatly by species. High settling velocities, up to 270 m d^{-1}, were determined for the large aggregates. Our results demonstrate that bacteria can substantially enhance gel particle coagulation and the formation of fast-settling large aggregates in seawater.

KEY WORDS: Bacteria · Bacterial community · Carbon cycle · Coagulation · Gel particle · Marine environment · *Pseudoalteromonas* · Settling velocity

INTRODUCTION

Gel-like particles, including transparent exopolymeric particles (Passow & Carlson 2012), submicron particles (Koike et al. 1990, Yamasaki et al. 1998), self-assembled microgels (Chin et al. 1998, Orellana et al. 2007), and other classes of polymeric particles (Mostajir et al. 1995, Long & Azam 1996, Samo et al. 2008), are ubiquitous in marine environments. These particles, which are generally thought to be highly porous and carbohydrate-rich (Verdugo et al. 2004, Passow & Carlson 2012), may dominate the particulate organic carbon (POC) pool in some oceanic regions (Passow 2002, Yamada et al. 2015). Verdugo et al. (2004) and Verdugo (2012) proposed a marine gel phase concept that emphasizes the role of the spontaneous assembly of dissolved polymers to form hydrogels: 3-dimensional polymer networks with a large free volume filled with seawater between polymer chains. This concept also provides a framework to describe the dissolved organic matter (DOM)–particulate organic matter continuum, covering the nanometer-to-centimeter size regime, in which the smaller gel particles are thought to serve as potentially important source particles that may stick together to form larger aggregates (Verdugo et al. 2004, Verdugo 2012, Jackson & Burd 2015). The large organic aggregates can play important roles in mediating the vertical delivery of organic carbon (Passow & Carlson 2012), serve as food for metazoans (Dilling & Brzezinski 2004, Newell et al. 2005), and provide microhabitats for microbes (Azam & Malfatti 2007). Consequently, a rigorous evaluation of the factors controlling gel particle coagulation is needed for a better understanding of particle dynamics and associated biogeochemical cycles in the oceans.

*Corresponding author: nagata@aori.u-tokyo.ac.jp

Publisher: Inter-Research · www.int-res.com

In general, particle coagulation in seawater is affected by particle abundance, collision rate constants, and particle stickiness (McCave 1984, Jackson & Burd 2015). The collision rate constants are described by coagulation kernels that are the functions of particle size and contain information on physical mechanisms (e.g. Brownian motion, fluid shear, and differential sedimentation) by which particles are brought together (Jackson & Burd 2015). The stickiness of particles determines the probability of adhesion after collision and is affected by several factors including the particle surface properties and physicochemical conditions of the ambient water (e.g. salinity, pH, and temperature; Johnson 1994, Gregory 2005). In marine environments, bacteria colonize organic particles and potentially influence the coagulation dynamics. While bacteria may promote the formation of large organic aggregates via the release of sticky extracellular polymers (Stoderegger & Herndl 1998, 1999, Sugimoto et al. 2007) and the stimulation of extracellular polymer excretion by diatoms (Gärdes et al. 2012), they can also disrupt large organic aggregates via ectoenzymatic hydrolysis of polymeric matrices (Azam & Malfatti 2007). These apparently conflicting roles of bacterial action may be partly explained by the involvement of different types of bacteria in aggregate formation and disintegration. Bacterial expression levels of carbohydrate-active proteins, including glycoside hydrolases and other outer membrane proteins, were reported to be taxonomically distinct (Teeling et al. 2012, Xing et al. 2015), suggesting that different groups of bacteria had specialized roles in polymer transformations. However, previous studies have generally focused on the degradation processes of polymers, with relatively little attention being paid to the relationship between bacterial metabolic capabilities and particle coagulation. Among the few existing studies is that of Ding et al. (2008), who suggested that a marine bacterium, *Sagittula stellat*e, excreted polymers to induce the formation of gel particles from DOM. However, to the best of our knowledge, whether marine bacteria and their specific taxonomic groups affect the coagulation of gel particles in seawater has not been studied.

To better understand the role of bacteria in the regulation of the marine gel phase, we investigated the effects of bacteria on the coagulation of gel particles composed of 2 polysaccharides (fucoidan and chitosan) derived from marine organisms. Fucoidan and fucose-rich polysaccharides are commonly found in brown seaweed and diatoms (Wustman et al. 1997, Morya et al. 2012), and chitosan is produced by the partial hydrolysis of chitin, a component of the exoskeletons of crabs, shrimps, and crustacean zooplankton (Rinaudo 2006). The constituents of fucoidan (fucose) and chitosan (*N*-acetyl-glucosamine) are abundant in marine environments (Borch & Kirchman 1997, Myklestad et al. 1997), and the functional groups of these polysaccharides (sulfate and amino groups in fucoidan and chitosan, respectively) are commonly found in gel-like polymers in marine waters (Long & Azam 1996, Stoderegger & Herndl 1998, 1999). Because the fucoidan/chitosan gel particles were ca. 100 µm in diameter (Yamada et al. 2013), the mechanisms of the formation and coagulation of the gel particles examined in the present study may differ from those of the nanogels (size, <200 nm) discussed by Chin et al. (1998), Verdugo et al. (2004), and Ding et al. (2007). Nonetheless, as described by Yamada et al. (2013), the fucoidan/chitosan gel particles had several key features of natural marine gels, including transparent exopolymer particles (Passow 2002), and were thought to provide important test cases relevant to marine microbial ecology and examples of bacteria–gel interactions in seawater. Our objectives were: (1) to investigate whether marine bacterial assemblages and their specific bacterial groups enhance the coagulation of gel particles, and (2) to determine the settling velocities of the large aggregates derived from gel particles.

MATERIALS AND METHODS

Collection of seawater samples and incubation of gel particles

Seawater samples were collected from the shore of Otsuchi Bay (39° 21′ 3″ N, 141° 55′ 58″ E) and Oarai Beach (36° 19′ 3″ N, 140° 35′ 29″ E) on the Pacific coast of northeastern Japan using a clean plastic bucket. Sampling dates and seawater properties (temperature and salinity) at the time of sampling are given in Table 1. Within 12 h of sampling, seawater samples were successively filtered through 0.8 and 0.2 µm pore size polycarbonate (PC) filters (47 mm diameter; Whatman) using negative pressure (<150 mmHg) to prepare filtered seawater with a pore size of 0.8 and 0.2 µm (hereafter $FSW_{0.8}$ and $FSW_{0.2}$, respectively). Portions of $FSW_{0.2}$ and $FSW_{0.8}$ were autoclaved for 15 min at 120°C and are hereafter referred to as Aclv-$FSW_{0.2}$ and Aclv-$FSW_{0.8}$, respectively. The gel particles were prepared using fucoidan and chitosan as previously described (Yamada et al. 2013; see the section 'Preparation of gel particles' in the Supple-

Table 1. Location and sampling date for each experiment, with seawater temperature and salinity at the time of sampling. A summary of the experimental setup (symbols indicate that the corresponding treatment was prepared [+] or not prepared [–]) and particle and bacterial parameters examined for each experiment are also given. N: nitrogen; P: phosphorus; A: particle abundance; S: size; V: settling velocity; BA: bacterial abundance; BCC: community composition; nd: not determined

Expt	Sampling date (dd/mm/yy)	Water temp. (°C)	Salinity	Bacteria-addition treatment			Sterile control	Parameters examined	
				No enrichment	P-enriched	P+N-enriched		Particles	Bacteria
Otsuchi Bay									
1	20/07/12	17.3	32.1	+	+	–	+	A/S	nd
2	26/07/12	21.1	30.8	+	+	–	+	A/S	nd
Oarai Beach									
3	07/02/13	18.2	28.2	+	+	–	+	A/S	BA
4	13/05/13	20.1	29.0	+	+	–	+	A/S	BA
5	12/08/13	24.1	24.3	–	+	+	+	A/S	BA/BCC
6	18/11/13	17.1	28.8	–	+	–	–	S/V	nd

ment at www.int-res.com/articles/suppl/a077p011_supp.pdf for detailed protocols). Briefly, 790 µl fucoidan (2.1% w v^{-1}, extracted from brown seaweed *Kjellmanialla crassifolia*) and 210 µl chitosan (3.8% w v^{-1}, extracted from snow crab *Chionoecetes opilo*) solutions were mixed in 50 ml Aclv-$FSW_{0.2}$ in a 50 ml polypropylene tube (at this stage, the formation of gel particles was observed), and the suspension was left at 4°C for 3 h. After removing the supernatant by aspiration (~10 ml solution remaining), 40 ml Aclv-$FSW_{0.2}$ was added to prepare the gel particle suspension. Note that because Aclv-$FSW_{0.2}$ was prepared using seawater that was collected at the time of each experiment (salinity range, 24.3–32.1), the chemical properties of Aclv-$FSW_{0.2}$ could differ depending on the experiment, which in turn might have affected the nature of the gel particles. However, the timing of gel formation and the abundance and size distribution of gel particles did not differ among experiments (data not shown), suggesting that the effect of the chemical variability of Aclv-$FSW_{0.2}$ on gel particle properties was small.

Five experiments were conducted to investigate the changes in particle abundance and mean volume in rotating tubes (Shanks & Edmondson 1989, Engel et al. 2009), with and without the presence of live bacterial assemblages of coastal seawater collected at either Otsuchi Bay (Expts 1 and 2) or Oarai Beach (Expts 3–5) (Table 1). An autoclaved 70 ml glass tube (No. 7L, 4.0 cm diameter and 7.5 cm length; AS ONE), with a cap sealed by a Teflon-faced nitrile-butadiene-rubber liner (25 mm diameter; Nichiden-Rika Glass), was filled with 56.18 ml of the gel particle suspension and 5.56 ml of either $FSW_{0.8}$ (bacteria-addition treatment) or Aclv-$FSW_{0.8}$ (sterile control). The concentration of the gel particles was adjusted to ca. 60 particles ml^{-1} (the actual initial particle concentration as determined by the method described in the section 'Particle abundance and size' was 58 ± 12 particles ml^{-1}, mean ± SD, n = 45). This initial gel particle concentration corresponded to 2.72 ± 0.47 mg C l^{-1} (mean ± SD, n = 9) in terms of POC concentration (determined for organic matter collected on pre-combusted [450°C for 4 h] glass-fiber filters [GF/F, nominal pore size 0.7 µm; Whatman] using an elemental analyzer [Flash 2000; Thermo Fisher Scientific]). This POC value lies within the higher range of POC levels previously reported for coastal and estuarine environments (Burney 1994).

In the following description of Expts 1–5, each treatment and control consisted of triplicate tubes. To examine the effects of nutrient addition on particle dynamics, we prepared a range of bacteria-addition treatments, with and without the addition of nutrients. In Expts 1–4, one treatment of bacteria-addition treatments received no nutrient enrichment, whereas the other treatment received phosphorus (P) enrichment (final concentration, 40 µM of Na_2HPO_4 solution). In Expt 5, the bacteria-addition treatment consisted of P enrichment, and P and nitrogen (N) (final concentration, 1.6 mM NH_4Cl solution) enrichment (Table 1). These nutrients were added to alleviate potential N and/or P limitation of bacteria that were fed with a carbon-rich substrate consisting of carbohydrates. At each sampling time (0, 24, 48, 72, and 96 h), 3 tubes for each bacteria-addition treatment and those for the sterile control were sacrificed to determine particle and bacterial parameters (Table 1). The rotation speed was adjusted to 16.4 rpm (Engel et al. 2009) using a rotator (ROLAA115S, Low Profile Roller; Stovall Life Science). The incubation was conducted at 20°C in the dark. Expt 6 was conducted to collect large aggregates for determination of settling velocities to infer the potential role of these aggregates in the vertical transport of materials.

Particle abundance and size

We used a digital camera (EOS Kiss X6i; Canon) equipped with a macro lens (EF5025M; Canon) and a converter lens (Life-Size Converter EF; Canon) to capture images of particles in the rotating tubes. The images were taken from the bottom of a tube that was laterally illuminated (mean beam depth, 5 mm) using a flashlight (SG-325; GENTOS). The center of each image (1.5 × 1.5 cm^2) was used as the sampling area. The depth at which the objects came into focus was determined to be 1.5 cm based on calibration using images of standard beads (Polystyrene Beads, Large [200–300 µm]; Polyscience). Depending on the treatment and the time of sampling, the particle abundance was occasionally too low to be detected in the sampling volume (<75 particles per tube). In this case, the rotating tube was removed from the roller, and particles were allowed to settle completely on the bottom of the tube (1–2 min). An image of particles on the bottom was then taken using a digital camera. The images obtained were analyzed using ImageJ software (v. 1.45 with Java, 1.6.0_20). Image analysis was conducted to estimate the area of individual particles. The resolution of the digital camera was 5184 × 3456 pixels (optical resolution 6.0 × 10^{-7} cm^2 per pixel), and the minimum particle size for image analysis (detection limit) was set at 2.0 × 10^{-5} cm^2 (33 pixels). The estimated area was converted to an equivalent spherical diameter (ESD) and volume, with the assumption that the particles were spherical.

Bacterial abundance

In Expts 3–5, seawater subsamples to determine bacterial abundance were fixed with glutaraldehyde (final concentration, 2%; Wako) for 1 to 2 h at 4°C. A portion of the fixed sample was first filtered through a 0.8 µm pore size syringe filter (Acrodisc syringe filter with Supor® membrane; Pall), and then the filtrate was further filtered through a 0.2 µm pore size PC filter (25 mm diameter; Whatman) to collect free-living bacteria. The other portion of the fixed sample was filtered through a 0.8 µm pore size PC filter (25 mm diameter; Whatman) to collect attached bacteria. After staining with 4,6-diamidino-2-phenylindole (DAPI; final concentration, 1 µg ml^{-1}; Porter & Feig 1980) for 5 min, the PC filters were mounted on slides using immersion oil (Vectashield, Vector Laboratories, and Citifluor) and then observed under an epifluorescence microscope (BX-61 equipped with a U-MWU2 cartridge; Olympus). At least 200 cells, or cells in 20 discrete fields, were counted for each slide.

Determination of bacterial phylogenetic composition by CARD-FISH

In Expt 5, the bacterial community composition was determined by the catalyzed reporter deposition fluorescence *in situ* hybridization (CARD-FISH) method (Pernthaler et al. 2004). Seawater samples were fixed with paraformaldehyde (final concentration, 2%; Wako) for 1 h at room temperature. The fixed $FSW_{0.8}$ was filtered through a 0.2 µm pore size PC filter. Other fixed samples were either filtered through a 0.2 µm pore size PC filter after prefiltration, using a 0.8 µm pore size syringe filter (Acrodisc syringe filter with Supor® membrane; Pall; free-living bacteria), or filtered directly through a 0.8 µm pore size PC filter (attached bacteria). The PC filters were dried and stored at −20°C for later processing. The PC filters were embedded in 0.1% agarose (Wako), cut into sections, and incubated in lysozyme (final concentration, 10 mg ml^{-1}; Sigma-Aldrich) for 1 h at 37°C. After inactivation of lysozyme by 0.01 M HCl at room temperature for 20 min, we performed hybridization with horseradish peroxidase-labeled oligonucleotide probes (Table S1 in the Supplement at www.int-res.com/articles/suppl/a077p011_supp.pdf) and tyramide (Alexa Fluor® 488) signal amplification. The filter sections were dehydrated with 95% ethanol and mounted on microscope slides using anti-fading reagents (Vectashield and Citifluor) containing DAPI (final concentration, 1 mg ml^{-1}; Sigma-Aldrich). Slides were stored at −20°C until later analysis. Slides were examined using an epifluorescence microscope (BX-61 equipped with U-MNIBA3 and U-MWU2 cartridges; Olympus).

Particle settling velocity and fractal dimension

The settling velocities of the large particles collected in Expt 6 (incubation period, 24–48 h) were determined using a sedimentation column (Ploug et al. 2010). A 1 l graduated cylinder (7 cm wide, IWAKI; AGC Techno Glass) was filled with $FSW_{0.2}$. After stabilization in a temperature-constant room (25°C), individual particles were gently introduced into the upper part of the water column using a micropipette (Finnpipette F2; Thermo Fisher Scientific), where the end of the tip had been sliced to broaden its opening. The travel time of individual particles (n = 45) over a distance of 20.5 cm (between 6 cm below the surface

and 6 cm above the bottom of the tube) was recorded using a manual stopwatch. Particles were placed in a Petri dish filled with $FSW_{0.2}$, and the lengths of their major and minor axes were determined using a ruler with the naked eye. The particle ESD was estimated assuming that the particles were ellipsoidal. Flexible large aggregates could be deformed after settlement on the bottom of the Petri dish, which might have resulted in an overestimation of the particle ESD. The effect of this potential error on the analyses of the relationship between the settling velocities and ESD was assumed to be minor.

To examine the geometric properties of organic aggregates produced during incubation, we estimated the fractal dimension (D_f) of aggregates on the basis of the power relationship between the settling velocities (U) and ESD (Logan & Wilkinson 1990, Logan & Kilps 1995). The constant (a) and exponent (b) of the power regression, which related U to ESD ($U = a \times ESD^b$), were estimated by nonlinear curve fitting (SigmaPlot 13.0; Systat Software) D_f was estimated using the following equation: $D_f = b + 1$ (Logan & Wilkinson 1990).

Effects of *Pseudoalteromonas* spp. isolates on particle dynamics

Pseudoalteromonas spp. isolates were obtained from the German Collection of Microorganisms and Cell Cultures (*P. agarivorans* [DSM14585], *P. rubra* [DSM6842], *P. tunicata* [DSM14096], *P. citrea* [DSM-8771], and *P. flavipulchra* [DSM14401]; Leibniz Institute DSMZ, Braunschweig, Germany), the Japan Collection of Microorganisms (*P. atlantica* [JCM8845], *P. luteoviolacea* [JCM21275], *P. haloplanktis* [JCM20767], *P. spongiae* [JCM12884], and *P. undina* [JCM20773]; RIKEN BioResource Center, Saitama, Japan), and the Belgian Coordinated Collection of Microorganisms (*P. ruthenica* [LMG19699]; BCCM/LMG Bacteria Collection, Gent, Belgium). The design of the incubation experiments was generally similar to that described for Expts 1–5, except for a few specific aspects including the use of artificial seawater, instead of $FSW_{0.2}$, for the preparation and incubation of gel particles (see the section 'Incubation experiments using *Pseudoalteromonas* spp. isolates' in the Supplement at www.int-res.com/articles/suppl/a077p011_supp.pdf).

Statistical analyses

Statistical comparisons of mean values were conducted after log transformation of the data so that they met the normality assumption, except for the maximum mean volume of particles (PV_{max}) value for the bacteria-addition treatment (P-enriched) in Expt 3 (this datum was not used for statistical analysis because the normality assumption was not met). After confirming homogeneity of variances in the data, we used 1-way ANOVAs followed by Holm-Sidak post hoc tests to compare PV_{max} values among the control and treatments (Expts 1–5). Next, because the data could not meet the assumption of homogeneous variances, we used Welch's t-tests to compare bacterial abundances (Expts 3–5) and Welch's ANOVAs followed by Games-Howell post hoc tests (Games & Howell 1976) to compare PV_{max} values among the control and *Pseudoalteromonas* spp. isolates (*Pseudoalteromonas* spp. experiments). Statistical calculations were performed using Microsoft Excel (Excel 2013; Microsoft).

RESULTS

Dynamics of particles and bacteria

Fig. 1 shows the time course of particle abundance, mean volume, and total particle volume (particle abundance × mean volume) in bacteria-addition treatments and the sterile control, with the results obtained in Expt 3 as an example. In the bacteria-addition treatment, particle abundance decreased by ca. 400-fold, and mean volume increased by ca. 10^5-fold during the incubation (Fig. 1A,B). Total particle volume also increased substantially (ca. 70-fold; Fig. 1C). In contrast, in the sterile control, the particle abundance, mean volume, and total particle volume changed only slightly during incubation (<1.5-fold difference; Fig. 1A–C).

The time course of particle coagulation is illustrated by a successive change in the particle size distribution during incubation (Fig. 2A). The size distribution of the particles initially added to the rotating tube had an ESD peak at the position of ca. 0.023 cm (see the graph at 0 h in Fig. 2A). The ESD peak position shifted toward larger size categories to reach the maximum size of ca. 0.832 cm at 96 h (Fig. 2A). In contrast, in the sterile control, there was a minimal shift in the ESD peak position during incubation (Fig. 2B).

A conspicuous formation of large aggregates in the bacteria-addition treatment, but not in the sterile control, was consistently observed in other experiments (Expts 1, 2, 4, and 5; Table 2). The PV_{max} values determined for the bacteria-addition treatment (PV_{max} was attained between 48 and 96 h) ranged

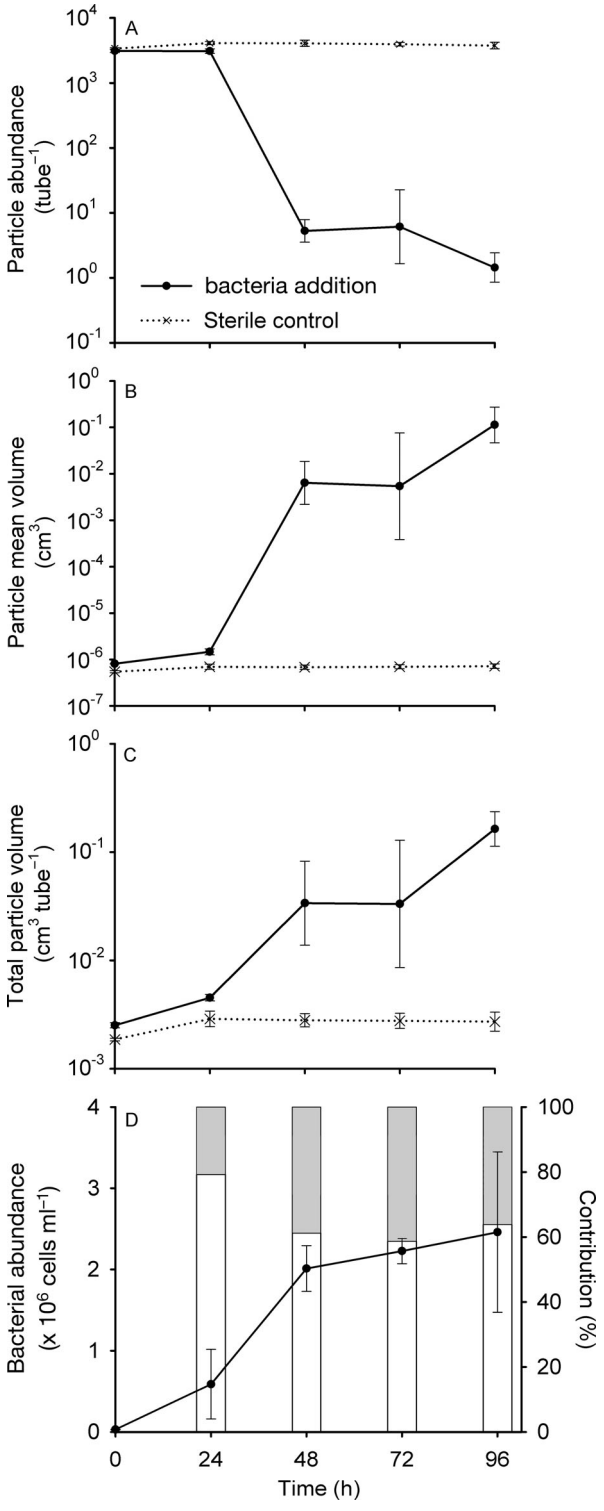

Fig. 1. Time course changes in (A) particle abundance, (B) particle mean volume, and (C) total particle volume. Panel (D) presents time course changes in bacterial abundance (solid line and symbols with errors for SD, n = 3) and the relative contribution of attached (open bar) and free-living (gray bar) bacteria to total bacterial abundance in the bacteria addition treatment in Expt 3. Bacterial abundances in the sterile control were low (1 × 10^2 cells ml^{-1}) and are not shown

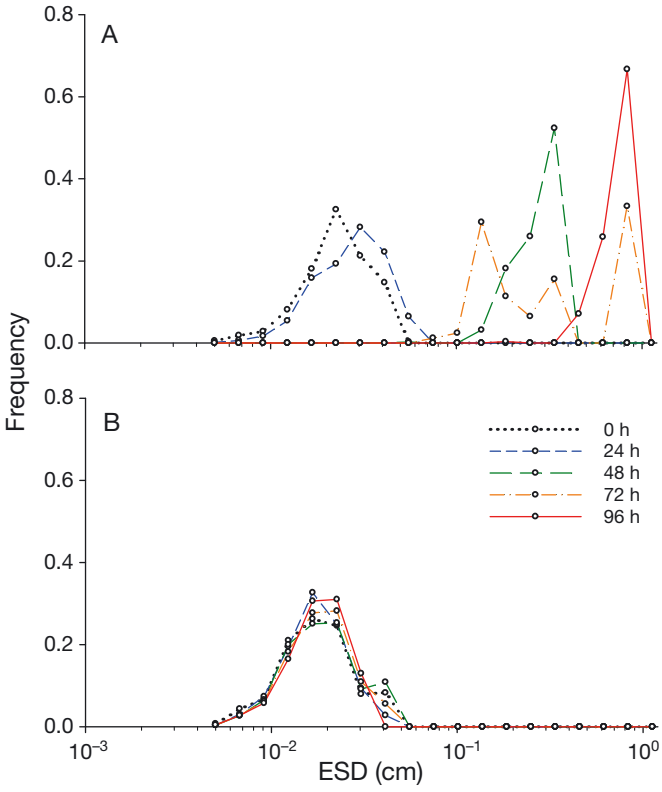

Fig. 2. Time course changes in aggregate size (equivalent spherical diameter, ESD) distribution (19 logarithmic bins are placed on the *x*-axis) in Expt 3 for (A) the bacteria-addition treatment and (B) the sterile control. The number of particles determined (n) was 9128 to 12 390 for the sterile control and for the initial sampling times (0 and 24 h) of the bacteria-addition treatment. n was 17, 33, and 5 for 48, 72, and 96 h, respectively, for the bacteria-addition treatment. The changes in aggregate abundance during the incubation are shown in Fig. 1

between 10^{-4} and 1 cm^3, which was 3 to 5 orders of magnitude greater than the value obtained for the sterile control in all experiments (Table 2). Among the bacteria-addition treatments, PV_{max} values increased by 20- to 110-fold in response to P enrichment in Expts 1 and 2, whereas the effect of P enrichment on PV_{max} was not significant in Expt 4. In Expt 5, the mean PV_{max} after P and N enrichment was significantly higher than in the P-enriched treatment (Table 2).

Changes in bacterial abundance were investigated in Expts 3–5 (Fig. 1D shows the results of Expt 3 as an example). Generally, the abundances of both the attached and free-living bacteria increased during the initial 24 to 48 h and then reached a stationary phase (bacteria attached to the gel particles were clearly seen under the epifluorescence microscope; Fig. S1 in the Supplement at www.int-res.com/articles/

Table 2. Maximum cell abundance and the maximum mean volume of particles (PV_{max}, mean ± SD, n = 3) in different treatments. Relative values of PV_{max} compared to that of sterile control were also tabulated. N: nitrogen; P: phosphorus; nd: not determined

Expt	Control/treatment	Max. cell abund. ($\times 10^5$ cells ml^{-1}) Mean	SD	p[a]	PV_{max} ($\times 10^{-6}$ cm^3) Mean	SD	PV_{max} relative to control[b] Mean	SD	Multiple comparison[c]
1	Sterile control	nd			1.2	0.3			1
	Bacteria-addition	nd			1.0×10^4	1.0×10^4	8.3×10^3	8.6×10^3	2
	Bacteria-addition (P-enriched)	nd			1.9×10^5	2.0×10^5	1.6×10^5	1.7×10^5	3
2	Sterile control	nd			0.9	0.0			1
	Bacteria-addition	nd			8.6×10^2	1.1×10^3	1.0×10^3	1.3×10^3	2
	Bacteria-addition (P-enriched)	nd			9.3×10^4	7.3×10^2	1.1×10^5	8.6×10^4	3
3	Sterile control	0.010	0.001		0.8	0.1			1
	Bacteria-addition	25	9.9		2.2×10^5	1.4×10^4	2.8×10^5	2.7×10^4	2
	Bacteria-addition (P-enriched)	45	9.6	0.075	1.7×10^5	1.3×10^5	2.3×10^5	1.7×10^5	not used[c]
4	Sterile control	0.014	0.002		5.0	0.7			1
	Bacteria-addition	35	18		1.7×10^5	1.1×10^5	3.5×10^4	2.2×10^4	2
	Bacteria-addition (P-enriched)	104	31	<0.05	2.2×10^5	2.5×10^4	4.3×10^4	8.0×10^3	2
5	Sterile control	0.026	0.003		4.3	0.4			1
	Bacteria-addition (P-enriched)	78	8.0		1.4×10^5	6.4×10^4	3.2×10^4	1.5×10^4	2
	Bacteria-addition (P+N-enriched)	127	26	0.066	3.1×10^5	2.8×10^4	7.2×10^4	9.5×10^3	3

[a]Welch's *t*-tests for the comparison between the means of different bacteria addition treatments
[b]PV_{max} of treatment/PV_{max} of sterile control. Error propagation was considered to derive SD
[c]ANOVAs with Holm-Sidak post hoc test. Different numbers indicate that the mean values were significantly ($p < 0.05$) different from each other in each experiment. The datum for the bacteria-addition treatment (P-enriched) in Expt 3 was not used for statistical analysis because normality assumption was not fulfilled

suppl/a077p011_supp.pdf). The abundance in the P-enriched treatments was significantly higher than that in the treatment without nutrient enrichment in Expt 4, whereas the difference was not significant in Expt 3 (Table 2). In Expt 5, the abundance after P and N enrichment did not differ significantly from that in the P-enriched treatment (Table 2).

The abundance of bacteria in the sterile control was 4.0×10^2 to 5.8×10^3 cells ml^{-1}, which did not change during the incubation.

Phylogenetic composition of the bacteria

CARD-FISH showed that at the level of the major phylogenetic group, *Bacteroidetes* was the most abundant group in the filtered seawater ($FSW_{0.8}$), followed by *Gammaproteobacteria* and *Alphaproteobacteria*. During the incubation, both attached and free-living bacteria displayed generally similar patterns of increase in terms of the changes in community composition (Fig. 3). The abundance of the *Bacteroidetes* group initially decreased (relative to $FSW_{0.8}$) drastically to <2% (at 24 h) before increasing to higher values (12–16%) at 96 h. During the whole incubation period, *Gammaproteobacteria* and *Alphaproteobacteria* (including the genus *Roseobacter*) were the predominant major phylogenetic groups. At a finer phylogenetic level (genus), there was a remarkable increase in the abundance of *Pseudoalteromonas* spp. (PSU730 probe-positive cells) during the early period of incubation. The *Pseudoalteromonas* spp. group accounted for only a minor fraction (2%) of the bacteria in the $FSW_{0.8}$, whereas it represented a substantial fraction (up to 28%) of bacteria at 24 h in both the attached and free-living bacterial fractions. The growth rate of this bacterial group during the initial 24 h was estimated to be 5.9 d^{-1} (attached bacteria) and 5.7 d^{-1} (free-living bacteria). These values were much higher than the corresponding growth rates of the bulk bacterial community (3.3 and 3.1 d^{-1} for attached and free-living bacteria, respectively). After 24 h, the abundance of this group remained high (9–25% of the total bacterial abundance; Fig. 3).

Effects of *Pseudoalteromonas* spp. isolates on particle dynamics

Based on our CARD-FISH results and other information regarding the general surface-associated lifestyle of *Pseudoalteromonas* spp. (see the section

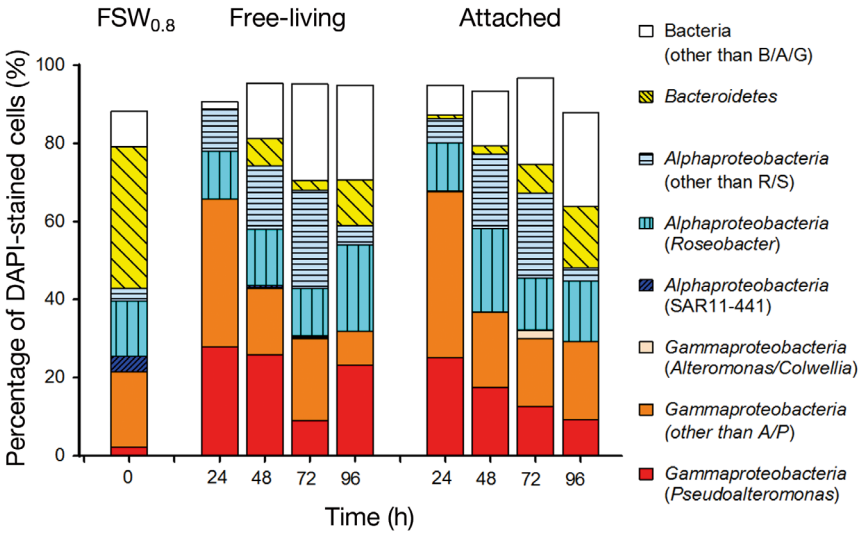

Fig. 3. Time course changes in the composition of phylogenetic groups for attached and free-living bacteria in Expt 5 (bacteria-addition treatment [phosphorus-enriched]). Values are the means of 3 tubes (coefficient of variation = 34.2 ± 36.6%, mean ± SD, n = 64) except for filtered seawater with a pore size of 0.8 µm ($FSW_{0.8}$, n = 2). The probes used for this analysis are in Table S1 in the Supplement at www.int-res.com/articles/suppl/a077p011_supp.pdf. The sum of the probe-positive cells did not add up to 100%, presumably because the catalyzed reporter deposition fluorescence *in situ* hybridization method failed to detect a fraction of the targeted cells (Amann & Fuchs 2008). B/A/G: *Bacteroidetes*, *Alphaproteobacteria* and *Gammaproteobacteria*; R/S: *Roseobacter* and SAR11-441; A/P: *Alteromonas/Colwellia* and *Pseudoalteromonas*; DAPI: 4,6-diamidino-2-phenylindole

Table 3. Maximum cell abundance and maximum mean volume of particles (PV_{max}, mean ± SD, n = 3) for different isolates affiliated with the genus *Pseudoalteromonas*. Relative values of PV_{max} normalized to that of the sterile control were also tabulated

Isolate	Max. cell abund. ($\times 10^5$ cells ml^{-1})		PV_{max} ($\times 10^{-6}$ cm^3)		PV_{max} relative to control[a]		p[b]
	Mean	SD	Mean	SD	Mean	SD	
Sterile control	0.004	0.006	1.1	0.2			
P. citrea	39	4.7	3.0×10^5	2.1×10^5	2.7×10^5	1.9×10^5	<0.05
P. luteoviolacea	18	4.8	1.3×10^5	8.3×10^4	1.1×10^5	7.6×10^4	<0.05
P. flavipulchra	13	1.4	180	90	160	83	<0.05
P. spongiae	9.3	2.7	31	14	28	13	<0.05
P. ruthenica	0.1	0.0	6.2	0.1	5.6	1.3	<0.05
P. undina	9.4	1.1	6.2	0.6	5.5	0.8	<0.01
P. atlantica	18	9.4	4.2	1.6	3.7	1.5	0.29
P. rubra	12	1.9	2.8	1.4	2.5	1.3	0.97
P. tunicata	11	0.8	1.9	0.9	1.7	0.8	0.99
P. haloplanktis	1.9	0.1	1.4	0.2	1.2	0.3	0.99
P. agarivorans	9.8	1.0	1.2	0.1	1.0	0.2	0.99

[a]PV_{max} of treatment/PV_{max} of sterile control. Error propagation was considered to derive SD

[b]Multiple comparisons of mean PV_{max} values among sterile control and treatments (isolates) were conducted using Welch's ANOVAs with Games-Howell post hoc tests. Statistical values for the significance of difference between treatment (each isolate) and sterile control are given

'Potential role of *Pseudoalteromonas* spp. in the enhancement of gel particle coagulation' in the 'Discussion'), we hypothesized that one type of bacteria that can enhance the formation of large organic aggregates is affiliated with the genus *Pseudoalteromonas*. To test this hypothesis, we examined 11 isolates of *Pseudoalteromonas* spp. to determine their effects to promote the formation of large aggregates from gel particles.

Pseudoalteromonas spp. isolates displayed high growth rates in particle suspensions, reaching a level of 9.3×10^5 to 39×10^5 cells ml^{-1}, except that the maximum cell abundances of *P. haloplanktis* and *P. ruthenica* were moderate (1.9×10^5 cells ml^{-1}) and low (0.1×10^5 cells ml^{-1}), respectively (Table 3). For 6 of the 11 isolates examined (*P. citrea*, *P. luteoviolacea*, *P. flavipulchra*, *P. spongiae*, *P. ruthenica*, and *P. undina*), the addition of the isolate resulted in a significant increase in particle mean volume relative to the sterile control (Table 3). Increases in particle volume were generally accompanied by decreases in particle abundance (data not shown), indicating that the coagulation of source particles was enhanced by the addition of these isolates. The extent of coagulation enhancement differed greatly among these isolates (Table 3). PV_{max} values determined for *P. citrea* and *P. luteoviolacea* were 1.1×10^5- to 2.7×10^5-fold higher than those in the sterile control. In contrast, the extent of enhancement in PV_{max} relative to the sterile control was only 5.5- to 5.6-fold higher for *P. ruthenica* and *P. undina*. *P. flavipulchra* and *P. spongiae* exhibited intermediate degrees of coagulation enhancement (28- to 160-fold higher than the control).

Settling velocity and fractal dimension of large aggregates

The large aggregates collected in Expt 6 were used to determine U (Fig. 4). U increased with increasing ESD, with values of 100 to 270 m d^{-1} obtained for the ESD class of 0.4 to 0.85 cm. The relationship between U and ESD was described by the following equation: $U = 318.0\ (\pm 16.6) \times \mathrm{ESD}^{0.823\ (\pm 0.067)}$ ($r^2 = 0.83$, $p < 0.001$, $n = 45$; errors are standard errors). Using the exponent of this regression equation, the fractal dimension, D_f, of large aggregates was estimated to be 1.82.

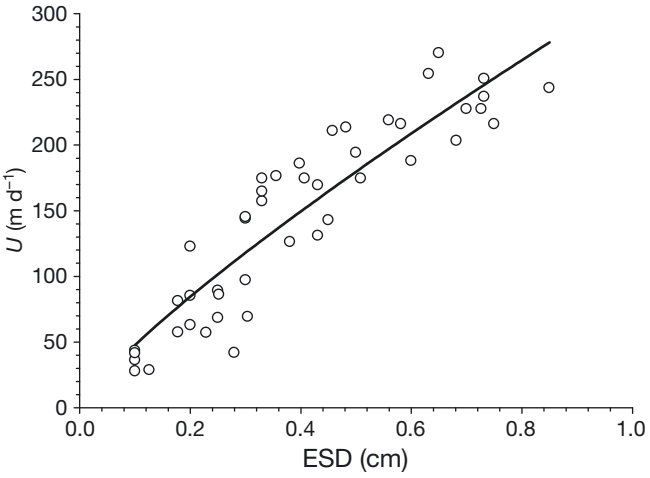

Fig. 4. Relationship between settling velocity (U) and equivalent spherical diameter (ESD) for the large aggregates collected from Expt 6. The line indicates the power regression obtained by nonlinear curve fitting $U = 318.0\ (\pm 16.6) \times \mathrm{ESD}^{0.823\ (\pm 0.067)}$ ($r^2 = 0.83$, $p < 0.001$, $n = 45$)

DISCUSSION

Enhancement of gel particle coagulation by marine bacteria

The addition of marine bacterial assemblages to gel particle suspensions resulted in a substantial increase (up to 10^5-fold) in particle mean volume, a reduction in particle abundance, and an increase in total particle volume during the incubation period of 24 to 96 h, with an accompanying increase in bacterial abundance. In contrast, in the sterile control, the gel particles displayed minimal changes in abundance and mean volume. The reduction in particle abundance and the increase in mean particle volume in the bacteria-added treatments could be explained by the coagulation. In our rotating tubes, the removal rate of the source gel particles due to coagulation can be described by:

$$\frac{\mathrm{d}C_n}{\mathrm{d}t} = -C_n \alpha_{nB} \beta_{nB} C_B - C_n \int_n^{\infty} (\alpha_{nm} \beta_{nm} C_m)\, \mathrm{d}m \qquad (1)$$

where C_n, C_B, and C_m are the concentrations of the source gel particles, bacteria, and the aggregates of gel particles, respectively; α_{nB} and α_{nm} are the stickiness (probability that 2 particles stick together following a collision event); and β_{nB} and β_{nm} are the collision rate constants (coagulation kernels), which are the function of particle size (Li et al. 2004, Jackson 2015). In our experiments (Expts 3–5), high bacterial abundance (high C_B) in the bacteria-added treatments (maximum abundances were on the order of 10^7 cells ml^{-1}) relative to that in the sterile control (10^2–10^3 cells ml^{-1}) indicates that collision events occurred much more frequently in bacteria-added treatments than in the sterile control. This implies that the removal of the source gel particle (decrease in C_n) due to the process denoted by the first term of the right-hand side of Eq. (1) was substantially enhanced by the addition and growth of bacteria. However, bacteria were much smaller than the gel particles (mean cell volume of bacteria was 0.68 μm^3 [data not shown], which was ca. 300-fold smaller than the mean volume of the gel particles initially added to the culture), and the total bacterial volume accounted for only 10% of the total volume of the source gel particles. Therefore, even if all the bacteria coagulated with the source gel particles, it is unlikely that the coagulation of gel particles and bacteria alone can explain the 10^5-fold increase in mean particle volume in the bacteria-added treatments. Alternatively, the gel particle coagulation rate could be enhanced due to the increase in the stickiness (α_{nm} in Eq. 1) of gel particles and aggregates in bacteria-added treatments. The attachment of bacterial cells on gel particles might result in alteration of gel particle surface properties, such as hydrophobicity, electric charges, and physical structures, which may in turn increase the stickiness to enhance particle coagulation. It is also possible that bacterial enzymatic cleavage of polymers may alter gel particle surface conformation, which may lead to the exposure of the residues or sites that promote adhesion.

There are other potential mechanisms by which bacteria promote gel particle coagulation or induce the increase in mean particle volume. Bacteria might release sticky polymeric particles into the ambient water (Stoderegger & Herndl 1998, 1999) and could also promote the conversion of DOM to nanogels (Ding et al. 2008). The production of these particles, which were not represented in Eq. (1), may affect

coagulation kinetics in rotating tubes. Furthermore, phase transitions of gels due to bacterial alteration of local physicochemical conditions might partially explain the changes in mean particle volume in rotating tubes. For example, a small shift in pH can cause a large change in gel particle volume due to swelling (Chin et al. 1998, Verdugo 2012). However, this mechanism alone would not explain the reduction in particle abundance during incubation.

Potential role of *Pseudoalteromonas* spp. in the enhancement of gel particle coagulation

The CARD-FISH results revealed that *Pseudoalteromonas* spp. grew rapidly during the initial phase of incubation when coagulation occurred. Their growth rates were much higher than the growth rate of the bulk bacterial community, which suggests that this group of bacteria was more competitive compared to the others, at least during the early phase of incubation. These results led us to hypothesize that one group of bacteria that played a role in the enhancement of gel particle coagulation was affiliated with the genus *Pseudoalteromonas*. This hypothesis is consistent with general knowledge of the physiological features of *Pseudoalteromonas* spp., some of which produce biofilms by excreting polysaccharides (Ortega-Morales et al. 2007) and have a strong surface attachment system (Hall-Stoodley & Stoodley 2002, Thomas et al. 2008). Our results obtained using the isolates of *Pseudoalteromonas* spp. strains not only support this hypothesis by showing that some isolates, including *P. citrea*, *P. luteoviolacea*, and *P. flavipulchra*, strongly enhance the coagulation of gel particles but also suggest that bacterial enhancement of gel particle coagulation is a species-specific trait (or group of traits). Given that the vast majority of bacteria in marine environments have yet to be cultured (Giovannoni & Stingl 2005), our isolate-based approach may have failed to identify the actual key players responsible for the enhancement of gel particle coagulation in natural environments. Nonetheless, our findings appear to offer a new perspective for developing a tractable approach to explore the detailed molecular basis of gel particle coagulation by means of comparative genetic and biochemical analyses among isolated bacterial strains. We emphasize the need for future studies to investigate a broader range of taxonomic groups and natural bacterial communities to identify the genetic traits, phenotypic characteristics, and molecular mechanisms involved in gel particle coagulation in marine environments.

Settling velocity of large aggregates

The settling velocities of the aggregates determined in this study (up to 270 m d^{-1}) were comparable to or exceeded those previously reported for various marine particles in a similar size range (0.1–1 cm), including marine snow (42–116 m d^{-1}; Alldredge & Gotschalk 1988), appendicularian house (8–71 m d^{-1}; Lombard & Kiørboe 2010), and laboratory-made aggregates containing mineral ballasts (34–357 m d^{-1}; Iversen & Ploug 2010). These data suggest that gel particle coagulation can potentially result in the formation of fast-settling aggregates. However, the validity of this assertion and the applicability of our findings to natural marine environments should be examined by future studies. As pointed out by Jackson (2015), in rotating tubes, large aggregates are formed under physical conditions that are largely different from those in oceans. Alldredge & Gotschalk (1988) claimed that the aggregates produced in rotating tubes could be compressed due to collision between aggregates and the wall, displaying a tendency toward faster settling speed. In contrast with their proposition, our estimate of D_f for large aggregates (1.82) was within the range of values previously reported for marine snow and other types of aggregates (1.26–2.14; Logan & Wilkinson 1990, Kilps et al. 1994), indicating that the large aggregates were porous with little indication of severe compression. However, it remains to be tested whether the physical and morphological characteristics of the large aggregates formed in rotating tubes represent the class of large particles found in natural marine environments.

Conclusions and future perspectives

Our data are among the first to demonstrate that the coagulation of self-assembled gel particles can be strongly enhanced by marine bacteria, adding to the previous proposition that bacteria can promote gel formation from DOM (Ding et al. 2008). In addition, our results obtained using various bacterial isolates suggest that the extent of gel particle coagulation enhancement is potentially a species-specific trait (or group of traits). Furthermore, we found that the settling velocities of large aggregates derived from the gel particles were high. These results have important implications for the refinement of the marine gel phase concept proposed by Verdugo et al. (2004) and Verdugo (2012), indicating the presence of a previously overlooked mechanism (i.e. species-specific

bacterial enhancement of coagulation or gel particle size) by which self-assembled gels can reach larger sizes. Future studies should identify the bacterial genetic traits and molecular mechanisms underlying gel particle coagulation enhancement. It is also important for future studies to investigate the general applicability of the results reported here to natural gel particles composed of different kinds of polysaccharides with different charges and polymer lengths.

Acknowledgements. This study was supported by JST, CREST and JSPS KAKENHI Grant Numbers 24241003 and 15H01725. Y.Y. was supported by JSPS research fellowships for young scientists and the Graduate Program for Leaders in Life Innovation (The University of Tokyo).

LITERATURE CITED

Alldredge AL, Gotschalk CC (1988) *In situ* settling behavior of marine snow. Limnol Oceanogr 33:339–351

Amann R, Fuchs BM (2008) Single-cell identification in microbial communities by improved fluorescence in situ hybridization techniques. Nat Rev Microbiol 6:339–348

Azam F, Malfatti F (2007) Microbial structuring of marine ecosystems. Nat Rev Microbiol 5:782–791

Borch NH, Kirchman DL (1997) Concentration and composition of dissolved combined neutral sugars (polysaccharides) in seawater determined by HPLC-PAD. Mar Chem 57:85–95

Burney CM (1994) Seasonal and diel changes in particulate and dissolved organic matter. In: Wotton RS (ed) The biology of particles in aquatic systems, 2nd edn. CRC Press, Boca Raton, FL, p 97–135

Chin WC, Orellana MV, Verdugo P (1998) Spontaneous assembly of marine dissolved organic matter into polymer gels. Nature 391:568–572

Dilling L, Brzezinski MA (2004) Quantifying marine snow as a food choice for zooplankton using stable silicon isotope tracers. J Plankton Res 26:1105–1114

Ding YX, Chin WC, Verdugo P (2007) Development of a fluorescence quenching assay to measure the fraction of organic carbon present in self-assembled gels in seawater. Mar Chem 106:456–462

Ding YX, Chin WC, Rodriguez A, Hung CC, Santschi PH, Verdugo P (2008) Amphiphilic exopolymers from *Sagittula stellata* induce DOM self-assembly and formation of marine microgels. Mar Chem 112:11–19

Engel A, Szlosek J, Abramson L, Liu Z, Lee C (2009) Investigating the effect of ballasting by $CaCO_3$ in *Emiliania huxleyi*: I. Formation, settling velocities and physical properties of aggregates. Deep-Sea Res II 56:1396–1407

Games PA, Howell JF (1976) Pairwise multiple comparison procedures with unequal n's and/or variances: a Monte Carlo study. J Educ Behav Stat 1:113–125

Gärdes A, Ramaye Y, Grossart HP, Passow U, Ullrich MS (2012) Effects of *Marinobacter adhaerens* HP15 on polymer exudation by *Thalassiosira weissflogii* at different N:P ratios. Mar Ecol Prog Ser 461:1–14

Giovannoni SJ, Stingl U (2005) Molecular diversity and ecology of microbial plankton. Nature 437:343–348

Gregory J (2005) Particles in water: properties and processes. CRC Press, Boca Raton, FL

Hall-Stoodley L, Stoodley P (2002) Developmental regulation of microbial biofilms. Curr Opin Biotechnol 13:228–233

Iversen MH, Ploug H (2010) Ballast minerals and the sinking carbon flux in the ocean: carbon-specific respiration rates and sinking velocity of marine snow aggregates. Biogeosciences 7:2613–2624

Jackson GA (2015) Coagulation in a rotating cylinder. Limnol Oceanogr Methods 13:194–201

Jackson GA, Burd AB (2015) Simulating aggregate dynamics in ocean biogeochemical models. Prog Oceanogr 133: 55–65

Johnson BD, Kranck K, Muschenheim DK (1994) Physicochemical factors in particle aggregation. In: Wotton RS (ed) The biology of particles in aquatic systems. CRC Press, Boca Raton, FL, p 75–96

Kilps JR, Logan BE, Alldredge AL (1994) Fractal dimensions of marine snow determined from image analysis of *in situ* photographs. Deep-Sea Res I 41:1159–1169

Koike I, Hara S, Terauchi K, Kogure K (1990) Role of submicrometre particles in the ocean. Nature 345:242–244

Li XY, Zhang JJ, Lee JH (2004) Modelling particle size distribution dynamics in marine waters. Water Res 38: 1305–1317

Logan BE, Kilps JR (1995) Fractal dimension of aggregates formed in different fluid mechanical environments. Water Res 29:443–453

Logan BE, Wilkinson DB (1990) Fractal geometry of marine snow and other biological aggregates. Limnol Oceanogr 35:130–136

Lombard F, Kiørboe T (2010) Marine snow originating from appendicularian houses: age-dependent settling characteristics. Deep-Sea Res I 57:1304–1313

Long RA, Azam F (1996) Abundant protein-containing particles in the sea. Aquat Microb Ecol 10:213–221

McCave IN (1984) Size spectra and aggregation of suspended particles in the deep ocean. Deep-Sea Res 31: 329–352

Morya VK, Kim J, Kim EK (2012) Algal fucoidan: structural and size-dependent bioactivities and their perspectives. Appl Microbiol Biotechnol 93:71–82

Mostajir B, Dolan JR, Rassoulzadegan F (1995) A simple method for the quantification of a class of labile marine pico- and nano-sized detritus: DAPI Yellow Particles (DYP). Aquat Microb Ecol 9:259–266

Myklestad AM, Skanoy E, Hestmann S (1997) A sensitive and rapid method for analysis of dissolved mono- and polysaccharides in seawater. Mar Chem 56:279–286

Newell CR, Pilskaln CH, Robinson SM, MacDonald BA (2005) The contribution of marine snow to the particle food supply of the benthic suspension feeder, *Mytilus edulis*. J Exp Mar Biol Ecol 321:109–124

Orellana MV, Petersen TW, Diercks AH, Donohoe S, Verdugo P, van den Engh G (2007) Marine microgels: optical and proteomic fingerprints. Mar Chem 105:229–239

Ortega-Morales BO, Santiago-Garcia JL, Chan-Bacab MJ, Moppert X and others (2007) Characterization of extracellular polymers synthesized by tropical intertidal biofilm bacteria. J Appl Microbiol 102:254–264

Passow U (2002) Transparent exopolymer particles (TEP) in aquatic environments. Prog Oceanogr 55:287–333

Passow U, Carlson CA (2012) The biological pump in a high CO_2 world. Mar Ecol Prog Ser 470:249–271

Pernthaler A, Pernthaler J, Amann R (2004) Sensitive multicolor fluorescence *in situ* hybridization for the identifica-

tion of environmental microorganisms. In: Kowalchuk GA, de Bruijn FJ, Head IM, Akkermans ADL, van Elsas JD (eds) Molecular microbial ecology manual, 2nd edn. Kluwer Academic Publishers, Dordrecht, p 711–726

Ploug H, Terbruggen A, Wolf-Gladrow D, Passow U (2010) A novel method to measure particle sinking velocity *in vitro*, and its comparison to three other *in vitro* methods. Limnol Oceanogr Methods 8:386–393

Porter KG, Feig YS (1980) The use of DAPI for identifying and counting aquatic microflora. Limnol Oceanogr 25: 943–948

Rinaudo M (2006) Chitin and chitosan: properties and applications. Prog Polym Sci 31:603–632

Samo TJ, Malfatti F, Azam F (2008) A new class of transparent organic particles in seawater visualized by a novel fluorescence approach. Aquat Microb Ecol 53:307–321

Shanks AL, Edmondson EW (1989) Laboratory-made artificial marine snow: a biological model of the real thing. Mar Biol 101:463–470

Stoderegger K, Herndl GJ (1998) Production and release of bacterial capsular material and its subsequent utilization by marine bacterioplankton. Limnol Oceanogr 43: 877–884

Stoderegger KE, Herndl GJ (1999) Production of exopolymer particles by marine bacterioplankton under contrasting turbulence conditions. Mar Ecol Prog Ser 189:9–16

Sugimoto K, Fukuda H, Baki MA, Koike I (2007) Bacterial contributions to formation of transparent exopolymer particles (TEP) and seasonal trends in coastal waters of Sagami Bay, Japan. Aquat Microb Ecol 46:31–41

Teeling H, Fuchs BM, Becher D, Klockow C and others (2012) Substrate-controlled succession of marine bacterioplankton populations induced by a phytoplankton bloom. Science 336:608–611

Thomas T, Evans FF, Schleheck D, Mai-Prochnow A and others (2008) Analysis of the *Pseudoalteromonas tunicata* genome reveals properties of a surface-associated life style in the marine environment. PLoS One 3:e3252

Verdugo P (2012) Marine microgels. Annu Rev Mar Sci 4: 375–400

Verdugo P, Alldredge AL, Azam F, Kirchman DL, Passow U, Santschi PH (2004) The oceanic gel phase: a bridge in the DOM-POM continuum. Mar Chem 92:67–85

Wustman BA, Gretz MR, Hoagland KD (1997) Extracellular matrix assembly in diatoms (Bacillariophyceae). I. A model of adhesives based on chemical characterization and localization of polysaccharides from the marine diatom *Achnanthes longipes* and other diatoms. Plant Physiol 113:1059–1069

Xing P, Hahnke RL, Unfried F, Markert S and others (2015) Niches of two polysaccharide-degrading *Polaribacter* isolates from the North Sea during a spring diatom bloom. ISME J 9:1410–1422

Yamada Y, Fukuda H, Inoue K, Kogure K, Nagata T (2013) Effects of attached bacteria on organic aggregate settling velocity in seawater. Aquat Microb Ecol 70:261–272

Yamada Y, Fukuda H, Uchimiya M, Motegi C, Nishino S, Kikuchi T, Nagata T (2015) Localized accumulation and a shelf-basin gradient of particles in the Chukchi Sea and Canada Basin, western Arctic. J Geophys Res Oceans 120:4638–4653

Yamasaki A, Fukuda H, Fukuda R, Miyajima T, Nagata T, Ogawa H, Koike I (1998) Submicrometer particles in northwest Pacific coastal environments: abundance, size distribution, and biological origins. Limnol Oceanogr 43: 536–542

Editorial responsibility: Craig Carlson, Santa Barbara, California, USA

Submitted: November 5, 2015; Accepted: March 1, 2016
Proofs received from author(s): April 18, 2016